Synthesis and Characterization of $Ni_{0.7}Mg_{0.3}Al_xFe_{2-x}O_4$ Mixed Magnetic Oxides with Spinel Struture

Dilipkumar.V.Meshram, Madhav N Rode, Uttam R. Kande

Abstract— The mixed magnetic materials (Ferrite) have been gaining importance in recent days especially in context of devices which can provide necessary infrastructure and flexibility for various human endeavrors. Materials are used in ultrasonic generators, modulators, phase-shifters and isolators, in memory recording devices for digital information etc. In present research work polycrystalline ferrite of composition $Ni_{0.7}Mg_{0.3}Al_XFe_{2-x}O_4$ with x = 0.0 to 0.5 has been successfully synthesized by conventional standard Ceramic method. The synthesized samples were processed into homogeneous powder form. The single phase cubic spinel structures of the samples were confirmed by X-ray diffraction patterns without any impurity peaks. Lattice constant is found to be decreasing with increase in Al^{3+} concentration in the composition (x). The X-ray density is found to be decreasing with increase of Al^{3+} concentration. The particle sizes lies between 300 ^{0}A to 450 ^{0}A. The porosity level is 0.20 to 0.30. The intensities of structure sensitive planes and ratios of intensities for selective places were used to propose the cation distribution. The infrared spectra of present series in range of 200 cm^{-1} to 800 cm^{-1} are taken. The IR spectra showed two absorption bands. The high frequency band v_1 (500cm^{-1}- 630 cm^{-1}) which is assigned to octahedral complex in spinel and low frequency band v_2 (390 cm^{-1} – 445cm^{-1}). The force constants have been obtained from infrared abosrpation data and its variation with respect to interstitial distance has been discussed. The saturation magnetization with increase in Al^{3+} content in the composition is studied. Thermoelectric power study exhibits that both n-type and p-type of charge carriers are responsible for charge transport and the drift mobility causes the conduction.

Index Terms — Ferrites, XRD, IR Spectra, Octabhedatal site, Tetrahedral site, Cation distribution.

1 INTRODUCTION

THE important innovations in the field of magnetic oxides took place after Second World War. The development of the magnetic oxides into useful materials has started by the pioneering work of late J.L.Snoek [1]. Since last five decades magnetic oxides have found increasing application in exacting technological requirements due to their controllable and combined magnetic and electrical properties [2]. Mixed magnetic oxides with spinel structure have wide technological applications. These are also known as ferrites if they have M^{2+} Fe_2^{3+} O_4^{2-} composition where M^{2+} is divalent metal ion. These materials are most relevant. The wide usefulness of these materials fascinated the scientists, physicists and engineers to study their basic properties in order to know the controllable parameters to design the suitable material for desired applications [3] The new findings with above approach may reveal the reality of controlling parameters and can lead to a breakthrough in the ferrite technology, which may be the most useful development. Thus mixed magnetic materials have been gaining importance in recent times especially in context of devices which can provide necessary infrastructure and flexibility for various human endeavors. Though various technological developments are taking place in fine tuning of these materials for specific attempts are still awaiting to explore the mysteries behind fascinating properties of mixed magnetic oxides.

- *Dr.Dilipkumar V Meshram, Vice-Principal, HOD, Department of Physics, Vaidynath College, Parli-Vai, Dist.Beed-431515,E-mail: dvmshram1164@gmail.com*
- *Madhav N Rode Asst.Prof. Department of Physics, Vaidyanath College, Parli-Vai, Dist.Beed-431515, India, Phone 02446-223555. E-mail: madhav_rode@yahoo.co.in*
- *Uttam R.Kande, Lecture in Physics,Department of Physics,Parli-Vai.*

Mixed magnetic oxides have novel combined electronic and magnetic properties. The most important thing about them are their high resistivity (from 10^{-3} Ωcm) [e.g. Fe2+Fe2+O42-] to 10^{11} cm [e.g. single crystalYIG.] wide useful range of magnetization, permeability and coercivity. These properties made them the most useful materials in science and technology. The properties like permeability and magnetic loss factor of material are of prime importance. In development of materials one aims at the best compromise between a high permeability and a low loss level. This can be achieved by suitable chemical composition, method of preparation and processing techniques. Thus the materials of vast range of promising properties have been developed and ferrites have become very useful in every walk of life in the modern world. Ferrites are widely used as core materials in transformers and in antenna of radio receivers as well as transmitters. They are used in ultrasonic generators, modulators, phase-shifters and isolators [4]. Some ferrites exhibit a typical rectangular hysteresis loop property. This rectangular hysteresis property and suitable coercivity are important factors to use ferrites in memory [5] and recording devices for digital information [6], Ferrites with small coercive force are used in magnetic amplifiers. Some hard ferrites are used in sound systems and in micro motors.

Ferrites with sharp and definite Curie temperature are used sensors of temperature controls. The position and rotational angle sensors have also been designed using ferrites. Radio waves absorbing point containing ferrites has been developed to render an aircraft or submarine invisible to radar. The pre-

cipitation of ferrite precurs is used to scavenge pollutant materials such as mercury from waste streams. Pollutants can be magnetically separated. Thus ferrites play important role in controlling pollution. The ferrites have been used as electrodes due to their high corrosion resistance and the appropriate conductivity. Ferrites are widely used in radio and television circuits. The largest consumption of soft ferrites is in television where half a kilogram is used for each set in the form of deflector and yoke. High frequency applications of soft ferrites include a large number of microwave components such as circulators, isolators, gyrators, phase shifters, YIG tuned filters, and switches and substrates for microwave integrated circuits. Some ferrites are used in switch mode power supplies. Thus ferrites have covered a vast area of applications.

Review of literate and aim of present investigation:-

Initially polycrystalline pure ferrites have been studied to know the controlling parameters behind basic properties. It is found that controllable properties of ferrites provide a wide scope of their technical applications. By suitable mixture of metal cations, ferrites with virtually any specific properties can prepared. Such mixed magnetic oxides are known as mixed ferrites. Many investigat0rs like E.W.Gorter and G.Blass had discovered the importance of mixed ferrites. The magnetic and electrical properties of such mixed ferrites depend upon method of preparation, atomic number and valence of metallic cation, stoichiometry of composition and sintering process (Sintering process includes rate of increase of sintering temperature, sintering temperature, rate of increase of sintering temperature, sintering temperature , rate of cooling after sintering for a certain duration and sintering duration).

The nickel ferrite ($NiFe_2O_4$) is an inverse spinel having a collinear ferromagnetic order [7]. The addition of trivalent ion like Al^{3+} and Cr^{3+} for Fe^{3+} in $NiFe_2O_4$ influences the electrical and magnetic properties of the system [8-14]. The investigation done by various worker have shown that the microstructure [15-17] electric [18-20], dielectric [21] and magnetic [22-25] properties of the basic nickel ferrite are greatly influenced when Ni^{2+} ions or Fe^{3+} ions are partially replaced by tetravalent ions. The most effective means to control saturation magnetization of nickel ferrite is through making substitution for trivalent iron. $NiAl_2O_4$ is a partially inverse spinel in which the ratio of Al^{3+} in the tetrahedral and octahedral site is about 2:3. $NiCr_2O_4$ is normal spinel with a canted ferromagnetic order at octahedral site [26].

The spinel structure seems to be particularly attractive as it allows a variety of magnetic orders from collinear to frustration. This is due to the fact that in spinels intra-sub-lattice interactions are weaker than the inter-sub-lattice interactions and as a result there are unsatisfied bonds increasing magnetic interactions accentuate the competition between the various exchange interactions resulting in a variety of magnetic structure [27]. The negative super-exchange interaction exists in ferrites. The strength of the exchange interaction is specified by exchange integral [28]. The exchange integrals of intra- sublattice interactions follow the order $J_{AB} > J_{BB} > J_{AA}$ in collinear ferrimagentic order. Thus the antiferromagetic A-B superexchange interaction is the main cause of the cooperative behavior in ferrites [29]. The magnetic order can be controlled by cation substitution [30]. It is found that change in J_{BB}/J_{AB} and M_A/M_B ratios modify the magnetic properties. This inspires to study the properties of ferrites with the substitutions of non-magnetic and magnetic cations. K.Seshen et al [31] have reported the effect of cation distribution on the properties of some magnesium-nickel ferrites in which the migration rate of Mg^{2+} on tetrahedral site depends upon the cooling rate of heat treatment due to high diffusibility.

The substitution of non-magnetic and magnetic cations with different valences on tetrahedral and octahedral sites has been a subject of many researchers in crystal lattice. The structure having collinear ferromagnetic order where degree of inversion depends upon the rate of heat treatment in preparation. Pure nickel ferrite is characterized by excessive losses. Therefore several investigators have proposed the substitutions of order cations. As with other ferrites, the most effective means to control saturation magnetization of nickel ferrite is through making substitution for trivalent iron. $NiAl_2O_4$ is partly inverse, $NiCr_2O_4$ is completely normal. Ni^{2+} cation has a strong octahedral site preference but nickel ferrite has been reported to be 80% inverse. Thus the system $Ni_{1-x}Mg_xFe_2O_4$ is expected to show variation in cation distribution on heat treatment and thereby the magnetization can be modified. Keeping nickel and magnesium in specific ration for which the magnetization will be maximum. The substitution of Al^{3+} as well as the substitution of Cr^{3+} may enhance basic properties of yielded mixed nickel ferrites.

In reported works to our knowledge, there is no mention of the studies of basic properties of the mixed magnetic oxides of solid solutions like $Ni_{0.7}Mg_{0.3}Al_xFe_{2-x}O_4$.

Therefore the studies of the basic properties of these mixed magnetic oxides with a view to study the effect of substitution of non magnetic and magnetic trivalent cations on the structural, electric and the magnetic properties have been undertaken for the present investigation.

2 Experiment Section

2.1 Sythesis of the system

The base system was synthesized to study its magnetization. The maximum saturation magnetization was considered to select the proportion of nickel and magnesium. The six samples of the system $Ni_{1-x}Mg_xFe_2O_4$ were prepared with x= 0.0 to 0.5 in the step of 0.1 using double sintering ceramic technique.

The starting materials were of analytical grade high purity oxides such as NiO, MgO and Fe_2O_3 (MERCK). They were taken in stoichiometric proportion by weighing with sensitive balance and were ground thoroughly. The pre-sintering is carried out using a programmable furnace namely Thermolyne

(Model-1500, USA made) at 900°C for 24 hours. The samples then were cooled slowly to room temperature. Pellets of 1 cm diameter of the powder have been made by cold pressing, applying the hydraulic pressure of 5 tones/inch^2. The good quality pellets have been obtained by using PVA as binder and maintaining the pressure for about ten minutes each time. The presintered pellets were again ground to fine powder. Then the powdered samples were pelletized again using hydraulic pressure machine by applying pressure of 5 tones/inch^2 and polyvinyl as binder. The pellets were finally sintered at 1050°C for 30 hours. Then they were cooled to room temperature at its natural rate.

The systems $Ni_{0.7}Mg_{0.3}Al_xFe_{2-x}O_4$ have been synthesized by the same ceramic technique. Six samples of each systems were prepared where x = 0.0 to 0.5 in step of 0.1. Here also AR grade oxides were used. The rest preparation process was similar to that of the base system.

2.2 Characterization

The Synthesis samples have been subjected to powder X-ray diffraction, IR spectra, Saturation magnetization, Thermoelectric power etc.

3 Result and Discussion

3.1 X-Ray Diffraction

The Single phase formation of all the samples was confirmed from X-ray diffraction pattern as shown in Figure (1 to 3). The values of the lattice parameter 'a' have been determined by using x-ray data with an accuracy of ± 0.002 A^0 for the samples having x = 0.0 to 0.5 and are listed in table 1. The variation of lattice parameter with increase of Al^{3+} concentration in the composition. Here is co-relation between the ionic radius and the lattice parameter. The ionic radii r_A and r_B have been estimated by considering the cation distribution. The values of theoretical lattice parameters have been determined by using the following relation [12].

$$a_{th} = \frac{8}{3\times\sqrt{3}}\left[(r_A + R_0) + \sqrt{3}(r_A + R_0)\right] \quad \text{……..(1)}$$

Where r_A and r_B are ionic radii of tetrahedral site and octahedral site respectively and R_0 is the radius of the oxygen ion [33]. The decrease in r_B with increase in Al^{3+} suggests the replacement of larger Fe^{3+} (0.64A^o) by smaller Al^{3+} (0.51A^o) [34] on B-site. The octahedral site plays a dominant role rather than the tetrahedral site in influencing the values of lattice parameter. The average ionic radii decrease slowly with increase in Al^{3+} content, which is reflected in the decrease in lattice parameter with (x). Thus the decrease in lattice parameter may be attributed to the replacement of larger ion Fe^{3+} (0.64 A^o) by Al^{3+} (0.51A^o). The values of the theoretical lattice parameter and the observed lattice parameter are listed in the table (2). The values of lattice parameter are found to be comparable with the reported values in the literature [35-36].

The X-ray densities of all the samples were calculated by using formula [37].

$$d_x = \left(\frac{ZM}{Na^3}\right) gm.cm^{-3} \quad \text{……..(2)}$$

Where a is lattice parameter, Z is number of molecules per unit cell (For spinel ferrite Z= 8), M is the molecular weight of the sample and Nis the Avagadro's number.

The particle size of all the samples was determined by Scherr's formula [38].

$$t = \frac{0.9\lambda}{\beta\cos\theta} \quad \text{……(4)}$$

Where t is particle size, λ is the wavelength of the target used (here CuKα=1.5418), β is the full width at half maximum of diffracted intensity line which is obtained by resolving (311) reflection line. The resolved peaks for all the samples are depicted in the Figure (1 to 6). The values of particle size is observed to be in the range 300A^o to 400 A^o and the mean particle size is estimated at 314.401 A^o. This is appreciably comparable value with that observed in ceramically prepared powders.

The percentage porosity (%P) of all samples has been determined with help of following relation [39].

$$\%P = \left[1 - \frac{d}{dx}\right]\times 100 \quad \text{…… (5)}$$

Where d is bulk density, dx is x-ray density. The values of %P are listed in the table (4.1). The porosity level is found to be 10% to 30%.The X-ray intensities have been calculated by using the formula given by Burger [40].

$$I_{hkl} = |F_{hkl}|^2 P.L_p \quad \text{…….. (6)}$$

Where F_{hkl} is structure factor, P is multiplicity and L_p is Lorentz polarization. The cation distributions are determined by considering the ratio of intensities for the structure sensitive planes [41-44]. According to Ohnishi and Teranshi [45] the intensity ratios of the planes $I_{(220)}/I_{(400)}$ and $I_{(422)}/I_{(400)}$ are structure sensitive. The ratios $I_{(220)}/I_{(400)}$ and $I_{(422)}/I_{(400)}$ have been taken into consideration to determine cation distribution besides the saturation magnetization. The intensity ratios are listed in the table (3). The cation distribution based on the X-ray intensity ratio has been estimated and it si given in table (3). The cation distribution based on the X-ray intensity ratio has been estimated and it is given in table (3).

Table 1. Variation of lattice parameter, X-ray density, particle size and porosity for $Ni_{0.7}Mg_{0.3}Al_xFe_{2-x}O_4$ System.

Composition (x)	Lattice Parameter		X-ray density dx.gm/cm^3	Particle size t. A^o	Porosity %
	$a_{obs.}$ A^o	$a_{cal.}$ A^o			
0.0	8.333	8.334	5.175	315.61	30
0.1	8.331	8.332	5.081	313.38	10
0.2	8.329	8.330	5.015	323.66	20
0.3	8.326	8.327	4.950	326.86	28
0.4	8.324	8.326	4.869	313.15	13
0.5	8.321	8.321	4.813	293.72	21

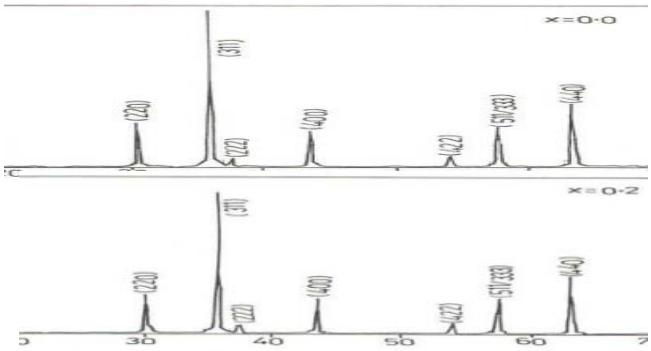

Figure 1:- XRD pattern for $Ni_{0.7}Mg_{0.3}Al_xFe_{2-x}O_4$; x =0.0; 0.1

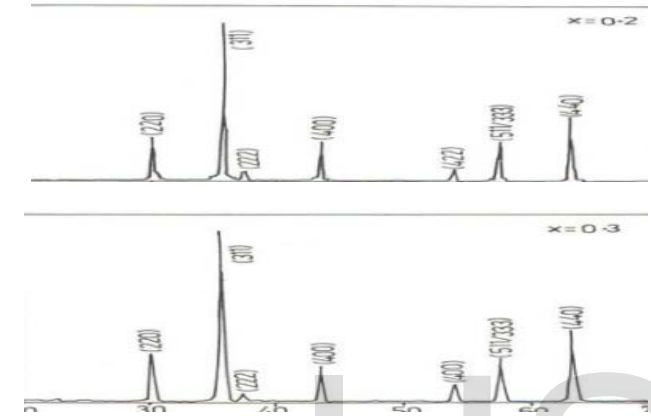

Figure 2:- XRD pattern for $Ni_{0.7}Mg_{0.3}Al_xFe_{2-x}O_4$; x =0.2; 0.3

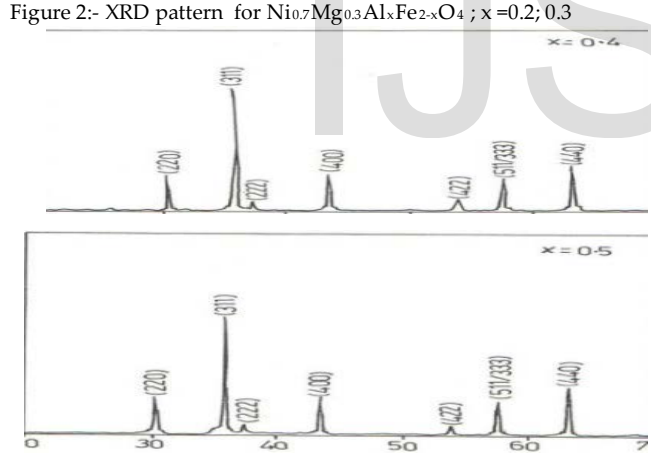

Figure 3 :- XRD pattern for $Ni_{0.7}Mg_{0.3}Al_xFe_{2-x}O_4$; x =0.4; 0.5

Table 2. Variation of ionic radii and lattice parameter (theoretical and observed) for $Ni_{0.7}Mg_{0.3}Al_xFe_{2-x}O_4$ System

Composition (x)	r_A A°	r_B A°	$a_{th.}$ A°	$a_{obs.}$ A°
0.0	0.64025	0.669425	8.323065	8.333
0.1	0.63742	0.664290	8.305169	8.331
0.2	0.68264	0.659820	8.286998	8.330
0.3	0.63120	0.655000	8.268971	8.328
0.4	0.66576	0.650780	8.250697	8.326
0.5	0.62280	0.645600	8.232819	8.319

Table 3 :- Cation Distribution and Intensity ratios for $Ni_{0.7}Mg_{0.3}Al_xFe_{2-x}O_4$ System.

(X)	Cation Distribution		Intensity Ratios					
	A-Sites	B-Sites	I_{220}/I_{400}		I_{422}/I_{400}		I_{440}/I_{422}	
			Cal.	Obs.	Cal.	Obs.	Cal.	Obs
0.0	$(Mg^{2+}_{0.015}Fe^{3+}_{0.985})$	$[Ni^{2+}_{0.7}Mg^{2+}_{0.285}Fe^{3+}_{1.015}]$	1.32	1.1	0.5	0.27	4.97	5.66
0.1	$(Mg^{2+}_{0.028}Al^{3+}_{0.022}Fe^{3+}_{0.95})$	$[Ni^{2+}_{0.7}Mg^{2+}_{0.272}Al^{3+}_{0.078}Fe^{3+}_{0.95}]$	1.36	0.90	0.5	0.27	4.56	4.76
0.2	$(Mg^{2+}_{0.038}Al^{3+}_{0.054}Fe^{3+}_{0.908})$	$[Ni^{2+}_{0.7}Mg^{2+}_{0.262}Al^{3+}_{0.148}Fe^{3+}_{0.892}]$	1.26	1.07	0.47	0.27	4.47	5.68
0.3	$(Mg^{2+}_{0.053}Al^{3+}_{0.081}Fe^{3+}_{0.866})$	$[Ni^{2+}_{0.7}Mg^{2+}_{0.247}Al^{3+}_{0.219}Fe^{3+}_{0.834}]$	1.21	1.08	0.46	0.31	0.46	4.44
0.4	$(Mg^{2+}_{0.065}Al^{3+}_{0.117}Fe^{3+}_{0.818})$	$[Ni^{2+}_{0.7}Mg^{2+}_{0.235}Al^{3+}_{0.283}Fe^{3+}_{0.782}]$	1.14	1.00	0.43	0.24	0.43	5.53
0.5	$(Mg^{2+}_{0.074}Al^{3+}_{0.138}Fe^{3+}_{0.788})$	$[Ni^{2+}_{0.7}Mg^{2+}_{0.226}Al^{3+}_{0.362}Fe^{3+}_{0.712}]$	1.13	1.04	0.43	0.17	0.43	6.94

3.2 IR Secptra

The IR Spectra of $Ni_{0.7}Mg_{0.3}Al_xFe_{2-x}O_4$, x = 0 to 0.5 in step of 0.1 systems are shown in the figure (4). The IR spectra of all samples have been used to locate the band position in order to determine the absorption frequency. The high frequency band ν_1 is in the range 600 to 610 cm^{-1} and the lower frequency band ν_2 is in the range 300 to 430 cm^{-1} [46-47]. The absorption bands obtained in the present investigation are found to be in the expected range of wave number. The difference in band position is expected because of the difference in the Fe^{3+}-O_2 distances for the octahedral and tetrahedral complexes. Waldron [48] and Hafner [49] attributed the ν_1 band to the instrinsic vibrations of the tetrahedral groups and ν_2 to the octahedral groups. The force constants have been calculated using the Waldron analysis. The bond lengths R_A and R_B have been determined using the formulate given Smith J.N. [50]. The values of K_t, K_O, R_A and R_B are listed in the table (4). The molecular weight at tetrahedral (M_t) and that at octahedral (M_o) site have been calculated using the cation distribution obtained from X-ray diffraction and magnetization measurements. The values of ν_1 , ν_2 K_t , K_o, R_A and R_B are found to be in good agreement with the reported ones. The force constant K_t decreases with the increase in R_A and the force constant K_o decreases with decrease in the R_B. The slight variations in ν_1 , ν_2 indicate that the method of preparation, grain size and sintering temperature can influence the band positions. The decrease in bond lengths is attributed to the decrease in lattice parameters. A slight splitting of some bands indicates valence variations of F_e. Normally the force constant for tetrahedral site is higher than that for octahedral site due to the stretching bond at tetrahedral site. The variation of K_t , K_o, R_A and R_B is

shown in figure (5-6).

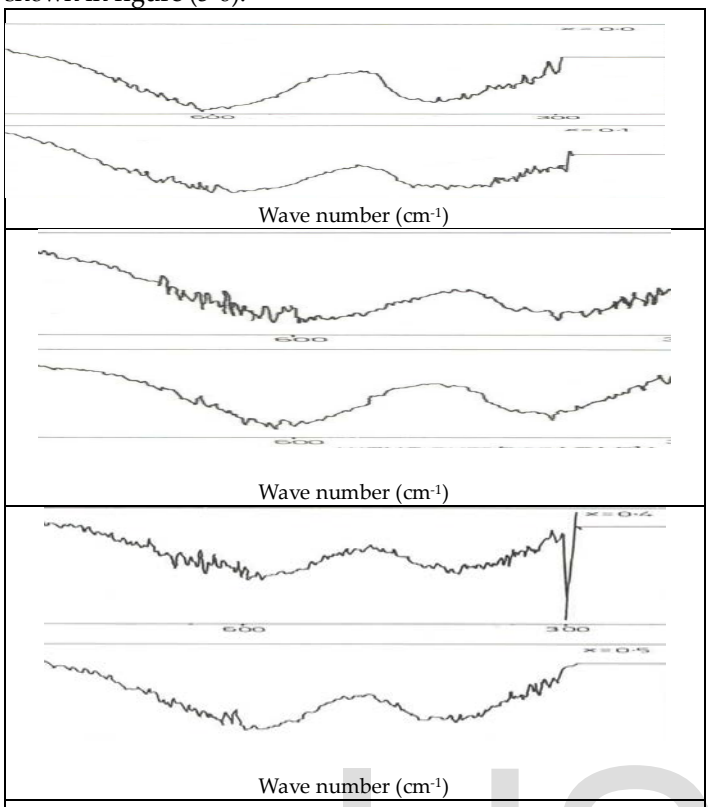

Figure 4 IR Spectra of $Ni_{0.7}Mg_{0.3}Al_xFe_{2-x}O_4$, x = 0.0 to 0.5

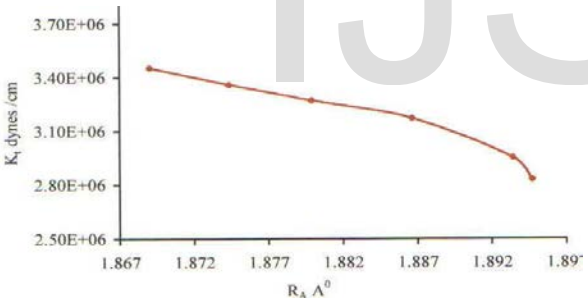

Figure 5

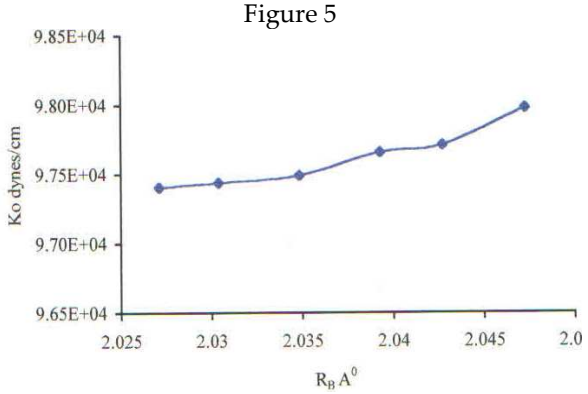

Figure 6

3.3 Saturation Magnetization

The values of saturation magnetization and Bohr magneton number (the saturation magnetization per formula unit in Bohr magneton) at 300⁰K were obtained from hysteresis loop technique for all the samples of the series (x=0.0 to x= 0.5). The observed and calculated magnetic moments for all samples are listed in the table (5). All the samples show decrease in η_B Al^{3+} content in the composition. The saturation magnetization σ_s is calculated from hysteresis loop for all the six samples and magnetic moment per formula unit is calculated by using the following relation [50].

$$\eta_B = \frac{\sigma_s}{555} \times M_{wt} \quad \text{.....(7)}$$

Where M_{wt} is molecular weight.

The decrease in the saturation magnetization with increase in Al^{3+} can be explained using Neel's [20] collinear model for ferrimagnetism. According to Neel's collinear model of ferrimagnetism, the magnetic moment per formula unit is expressed as

$$\eta_B^N = M_B(x) - M_A(x) \quad \text{.....(8)}$$

Where $M_A(x)$, $M_B(x)$ are magnetic momnts in of sublattice A and B respectively. The theoretical values of magnetic moment per formula unit in Bohr's magneton η_B^N have been estimated by using the cation distribution. The η_B^N values for $Ni_{0.7}Mg_{0.3}Al_xFe_{2-x}O_4$ x= 0 to 0.5 , were calculated by using the ionic magnetic moments of Fe^3 , Ni^{2+}, Mg^{2+}, Al^{3+} with their respective values $5\mu_B, 2\mu_B, 0\mu_B, 0\mu_B$. The experimental and calculated values of η_B^N have been given in the table (5). The variation of η_B^N with respect to the Al^{3+} concentration in the composition is shown in figure (7). The curves suggest the collinear spin order in the samples, which indicate a strong A-B interaction even though the non-magnetic cation is substituted [52-53].

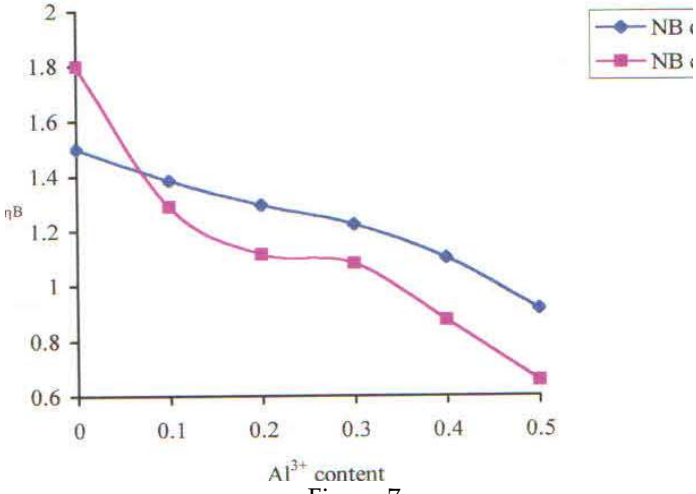

Figure 7.

Table 4. Vibration frequency, Bond lengths and force constant for $Ni_{0.7}Mg_{0.3}Al_xFe_{2-x}O_4$ System.

(X)	Vibration Frequencies		Bond Lengths		Force Constants	
	ν_1	ν_2	R_A A°	R_B A°	$K_t \times 10^5$	$K_t \times 10^5$

	cm^{-1}	cm^{-2}			dynes/cm	dynes/cm
0.0	610	405	1.869042	2.047287	3.511480	0.97976
0.1	610	400	1.874365	2.042744	3.357251	0.97706
0.2	590	400	1.879911	2.039302	3.052872	0.97656
0.3	610	410	1.886672	2.034842	3.169458	0.97486
0.4	600	400	1.893429	2.030397	2.975550	0.97432
0.5	600	400	1.894719	2.027117	2.828725	0.97401

Table 5. Saturation magnetization Bohr's magneton and Curie temperature for $Ni_{0.7}Mg_{0.3}Al_xFe_{2-x}O_4$ System.

(X)	Saturation Magnetization σ_s (emu/gm)	η_B (μ_B)		Curie Temperature T_c (^{0}K)	
		Cal.	Obs.	From Susc.	From d.c. Resty.
0.0	37.294	1.55	1.496	819	809
0.1	34.882	1.40	1.381	802	790
0.2	33.11	1.32	1.294	794	780
0.3	31.702	1.24	1.222	780	750
0.4	31.334	1.22	1.1	770	740
0.5	26.852	1.02	0.913	762	720

3.4 Thermoelectric Power

The thermoelectric power measurement of all the samples have been carried out from room temperature to 850 ^{0}K temperature. The values of Seebeck coefficient (α) have been determined by using the following relation.

$$\alpha = \frac{Thermo\ emf}{Temrature\ difference\ across\ the\ sample} \quad \text{.....(9)}$$

The plots of Seebeck coefficient as a function of temperature are shown in the fig (8-9). The Seebeck coefficients have been observed to be negative upto 530^{0}K and later on positive for higer temperature for all samples. This indicates that both type of charge carriers are present in the system. The α decreases nonlinearly with increase in temperature. At high temperature number of holes hopping between Ni^{3+} to Ni^{3+} may increase which give rise to positive Seebeck coefficient [54]. The charge carrier concentration has been determined by using the following relation,

$$n = Nexp\left(\frac{-\alpha}{\kappa}\right) \quad \text{.....(10)}$$

Where N is the density of the state and k is Boltzmann constant. The variation of concentration of charge carrier with temperature is as shown in figure (10-11)

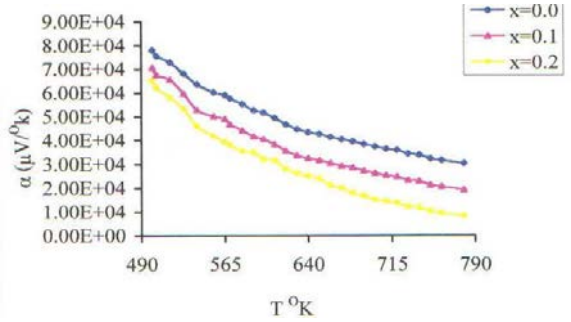

Figrue 8

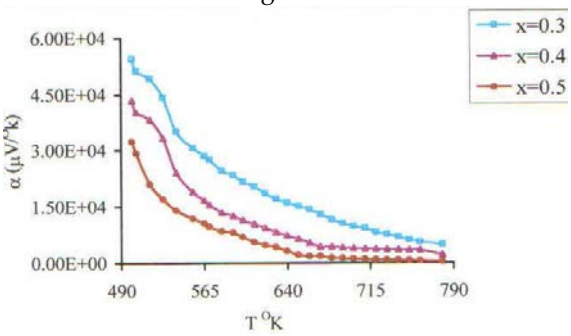

Figrue 9

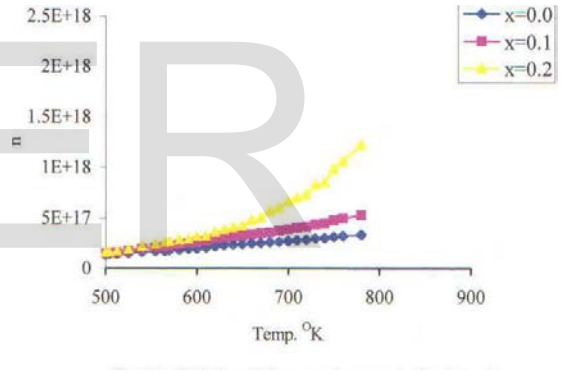

Figure 10

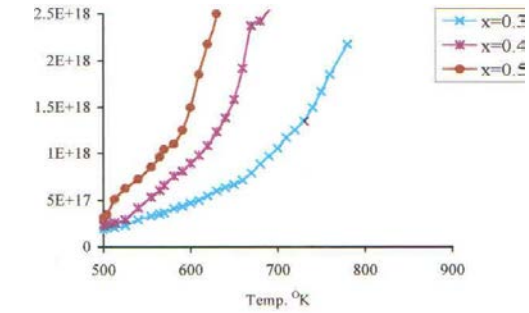

Figrue 11

The concentration of the charge carries increases with the increase in temperature. The mobility for all the samples has been calculated by the following relation,

$$\mu_d = \frac{\sigma}{ne} \quad \text{.....(11)}$$

Where σ is dc conductivity, η is concentration of charge carriers and e is electronic charge. The variation of drift mobility with temperature is as shown in figure (12- 13). The drift mo-

bility increases with increase in temperature and decreases with Al^{3+} content. This clearly indicates that the conduction in the systems depends on the temperature dependent drift mobility and not on the temperature dependent charge carrier concentration. The Seebeck coefficient for the present series show that initially n-type region is due to electron hopping Fe^{2+}=> Fe^{3+} and that in p –type is due to hole transfer between the two different valence states of the cation. Both Al^{3+} and Ni^{2+} may be playing certain role in controlling the resistivity along with Fe^{2+}- Fe^{3+} pair . From the thermoelectric power the conduction is observed depending on the temperature dependent drift mobility and not the temperature dependent charge carrier concentration [55].

4 Conclusion

Thus from the above results and discussion the following conclusions can be drawn.

1. $Ni_{0.7}Mg_{0.3}Al_xFe_{2-x}O_4$ system has spinel structure.
2. The substitution of Al^{+3} decreases the lattice parameter.
3. The infrared spectra of the system consist of two bands, which correspond to the intrinsic vibrations of tetrahedral and octahedral complexes.
4. The force constant K_t decresases with increase in bond length R_A.
5. The force constant K_o decreases with decreases in bond length R_B.
6. The saturation magnetization decreases with increase in Al^{3+} content in the composition. The variation of the saturation magnetization obeys the Neel's two sub lattice collinear model for ferrimagnetism. The substitution of non-magnetic Al^{3+} ion does not disturb the A-B interaction. But it decreases the pair of interaction Fe^{3+} -O- Fe^{3+} at B site modulate saturation magnetization by occupying more at B-site as compared to that at A-site.
7. The variation of ac susceptibility with increase in temperature indicates the normal ferromagnetic behavior of the system. The system has multidomain structure.
8. The Curie temperature decreases with increase in the Al^{3+} in the composition.
9. The dc resistivity increases with increase in Al^{3+} content in the composition.The behavior of the system changes from ferromagnetic to paramagnetic at aparticular temperature.
10. Thermoelectric power study exhibits that both n-type and p- types of charge carriers are response/ble for charge transport and the drift mobility causes the conduction.

References

[1] J.L.Snock, Physica,3 (1936) 463.
[2] K.J.Standley, Oxide Magnetic Material Clarendon press, Oxford (1962)
[3] Alex Goldman, Modern Ferrite Technology, Van Nostrand Reinhold, New York (1990)
[4] R.F.Soohoo, Microwave magnetic, Harper & Row Publishers New York (1985)
[5] R.S.Weiss, Phys. Rev. 96 (1954) 800.
[6] I.Stein,J.Appl. Phys.,34, 7, 1976 (1963).
[7] J.M.Daniel, A.Rosenwaig, Can. J.Phys.,48 (1970)381.
[8] T.Tsushima Jr.Phys.Soc. Japan 18 (1963)1162.
[9] J.J.Bar, A.T.Pedziwiatr, Z.M.Standnik, A.Szytwa, J.Todorovic, Z. Tomokowez,W.Zarek,phys.stat.Sol.A44(1977)325.
[10] L.R.Maxwell, S.J.Piceart, Phys. Rev.92(1953)1120.
[11] A.Hauet, J.Teillet, B.Hannoyer, M.Lenglet, Phys. Stat.Sol.A103 (1987) 1257.
[12] J.Chappert,R.B.Frankel, Phys. Rev.Lett.19(1967)570.
[13] V.I.Nikoloev et.al,Sov.,Phy.Solid state 13(1971)317.
[14] V.I.Nikooev et.al.,Sov.,Phy.Solid State 14(1972)521.
[15] J.S.Baijal, D.Kothari, S.Phanjauban, Solid State. Commun .69(1989)277.
[16] D.C.Khan, M. Mistra. A.R.Das,Jr.Appl. Phys.5 (1982)2722.
[17] B.V.Bhise, M.B.Dongare, S.A.Patil, S.R.Sawant, Jr.Mater.Sci.Lett.10 (1991) 922.
[18] B.L.Patil, S.R.Sawant, S.A.Patil,R.N.Patil, Jr.Mater.Sci.29(1994) 175.
[19] M.G.Patil, V.C.Mahajan, S.D.Latke, B.V.Bhise & S.A.Patil, Solid State.Commun. 91(1994) 667.
[20] C.Prakash, J.S.Baijal, P.Kishan, Jr.Less.Common.Met.106 (1985) 257.
[21] C.Praksh, J.S.Baijal, P.Kishan, Jr.Less.Common.Met. 107(1985) 51.
[22] S.Unnikrishnan, D.K.Choundhary, Phys .State. Sol(a) 121(1990) 265.
[23] H.N.Padys, R.G.Kulkari, Solid State. Commun .61(1987)645.
[24] C.Prakash,Jr. Mater. Sci.Lett.6 (1987)504.
[25] A.R.Das,V.S. Anathan, D.C.Khan,Jr.Appl.,Phys.57 (1985) 4181.
[26] T.A.Kaplan, K.D wight, D.Lyons & N.Menuyk, Jr.Appl. Phys. 32(1961)135.
[27] N.N.Jani, B.S.Trivedi, .H.Joshi, G.K.Bichile & R.G.Kulkarni, Bull.Mater.Sci.Vol.21, No.3, June (1998)233-239.
[28] E.W.Gorter Proc .I.R.E.43 (1955)1945.
[29] P.W. Anderson, Phys.Rev.79 (350)350.
[30] Y.Yfet & C.Kittel., Phys.Rev.87 (1952)290.
[31] K.Seshan, A.L.Shashimohan, D.K.Chakrabarty & A.B.Biswas, Phys.State.Sol 68 (1981)97-101.
[32] Mazen S.A., Abdalla M.H., Nakhla R.I., Zaki H.M. & Metawe F., Bull. For Sci. Zagasig Uni.13 (1991)344.
[33] Mazen S.A., Abdalla M.H., Sabrah B.A.& Hashem H.A., M.Phys. Status solidi, A 134 (1992)263.
[34] Dunitz J.D., Orgel L.E., J.Phys. Chem. Solids(1957)
[35] Kunal B. Modi, et.al, Jr. of Materials Sci. Letters 17 (1998).
[36] Kunal B Modi, et.al, Jr. of Materials Sci. 31 (1996) 1311.
[37] Cullity B.D., Elements of X-ray Diffraction (Addison Wesley Press Reading M.A. (1959).
[38] Standley K.J., Oxide Magnetic Materials Clerenden Press, Oxford,(1972).
[39] Buerger M.J. , Crystal structure Analysis., Wiley New York (1960).
[40] R.K.Datta, R.Roy , Jr. Am. Cerm. Soc. 50 (1967) 578.
[41] R.W.G.Wyckoff, Crystal Structure., Vol.2, P-75, Interscience, New York (1964)
[42] E.W.Gorter Philips Res. Rep.9, 295 (1954).
[43] E.F.Bertaut, C.r.hebd Seanc.Acad.Sci.Paris 230,213 (1950)
[44] E.F.Bertaut, Jr.Phys.Rad.,12, 252(1951).
[45] Ohnishi & Teranishi T.,JR.Phys.Soc.,Jpn.,16 (1961),36
[46] Preudhomme J. & P.Tarte, Spectrochim Acta 28 A(1972) 69.
[47] P.Tarte, Spectrochim Acta 19 (1965)49.
[48] R.D.Waldron Phys.Rev.99 (1955)1727
[49] S.T.Hafner Z. Fur Krist 115,(1961) 331.
[50] J.N.Smith, Magnetic properties of material Mc Graw-Hill, New York.
[51] L.Neel, Ann.Phys.3 (1948)137.
[52] Urvi V.Chhaya, Bimal S. Trivedi et al. Physica B. 262 (1999) 5-12.
[53] K.B.MOdi et al Jr. of material Science 34 (1996) 1311-1317.

[54] D.Ravinder, G. Ranga Mohan, Material letters 44 (2000) 139-143.
[55] P.V.Reddi and T.S.Rao, Phys. Stat.,Solid State sol(a)91,303(1985)